VILNIUS UNIVERSITY
FACULTY OF CHEMISTRY AND GEOSCIENCES
DEPARTMENT OF INORGANIC CHEMISTRY

Sonia Ishioma Okolo
Main study program Pharmaceutical Chemistry
Master Thesis

STUDY ON THE STRUCTURE AND ELECTROCATALYTIC ACTIVITY TOWARD HYDROGEN PEROXIDE OF GRAPHENE-BASED NANOCOMPOSITE MATERIALS CONTAINING ORGANIC DYES

Supervisor
Dr. Justina Gaidukevič

_____
(permission to defend, date, signature)

Co-supervisor:
Dr. Julija Razumienė

_____
(permission to defend, date, signature)

Date of submission _____
Registration number _____

Vilnius 2021

CONTENTS

ACKNOWLEDGEMENT

To Dr. Justina Gaidukevi and Dr. Jurgis Barkauskas, my supervisors who deserve special thanks for their direction, comments, contributions, and recommendations during this study. I'd like to express my gratitude to Dr. Julija Razumiené and Viduté Gurevičiene for their invaluable assistance with electrochemical analysis. I'd like to thank Dr. Tomas Murauskas for providing XPS measurement. To my friends for their encouragement and unwavering support and to my loving family for giving me the opportunity to fulfil my dream.

INTRODUCTION

Graphene is a 2D atomic-scale material made up of sp^2 hybridized carbon atoms that are arranged in a hexagonal lattice to form a honeycomb-like structure. In 2004, graphene was first separated from graphite by simple mechanical peeling method by Novoselov and Geim (Nobel Prize in Physics, 2010) [1]. Graphene oxide (GO) is the product of chemical exfoliation and oxidation of layered crystalline graphite. Remarkably, carbon atoms in GO maintain their integrity under specific conditions (2D structure). Similar to graphene, GO is a 2D structure containing certain oxygen functional groups (mostly epoxy- and hydroxy-) on its surface [2]. In 1859, Benjamin Brody first synthesized GO [3]. The method of synthesis involved oxidation with $KClO_3$ and exfoliation of natural crystalline graphite. Some other oxidizers were later proposed ($KMnO_4$; Hummer [3]) that simplified the synthesis of GO.GO can be used as a precursor in the synthesis of graphene of graphene-like materials (reduced GO; rGO). rGO can be produced from GO via chemical, thermal or UV-assisted methods [4]. GO unlike graphene, is quite strongly hydrophilic due to the presence of oxygen – containing functional groups. The hydrophilicity of GO is highly valued in the production process of graphene and graphene-like materials. For that purpose, graphene is widely used in the manufacturing of functional films and coatings, supercapacitors and battery electrodes, fuel cells, etc. In medicine GO is applied as drug carrier and anti-microbial material [5]. In chemistry, biology, pharmacology, and environmental conservation, determining hydrogen peroxide is critical. Titrimetry, fluorimetry, spectrophotometry, chemiluminescence, and electrochemical sensors are just a few of the techniques used to detect hydrogen peroxide. Except for electrochemical sensors, the majority of them are expensive and time-consuming [6,21]. The aim of this work is to produce graphene oxide/ organic dyes nanocomposites and to investigate their sensitivity in the non-enzymatic detection of hydrogen peroxide.

The task of this study were formulated as follows:

1. To synthesis GO and GO/dye (GO/congo red, GO/neutral red and GO/malachite green) nanocomposites.
2. To characterize prepared samples by SEM, Raman spectroscopy, FTIR and XPS analysis methods.
3. To evaluate prepared nanocomposites materials in terms of electrocatalytic performance for H_2O_2 detection.

LIST OF ABBREVIATIONS

GO – Graphene Oxide
ROS – Reactive Oxygen Species
Pt NP – Platinum nanoparticles
CNT – Carbon nanotube
MWCNT- Molecular weight carbon nanotube
MG - Malachite green
NR- Neutral red
CR- Congo red
AA – Ascorbic acid
UA - Uric acid
EDTA- Ethylenediaminetetraacetic acid
rGO- reduced graphene oxide
DNA- Deoxyribose nucleic acid
SOD- Superoxide dismutase
CuO- Cupper oxide
LOD- Limit of detection

1. LITERATURE SURVEY

1.1. Functionalization of GO surface

There is no precise agreement between scientists about the structure of GO. The LerfKlinowski model [7] is widely recognized and has formed the basis of much scientific research. This model assumes a random distribution of epoxy and alcohol groups on the surfaces, with alcohol and carboxyl groups around the edges, as shown in Fig. 1.

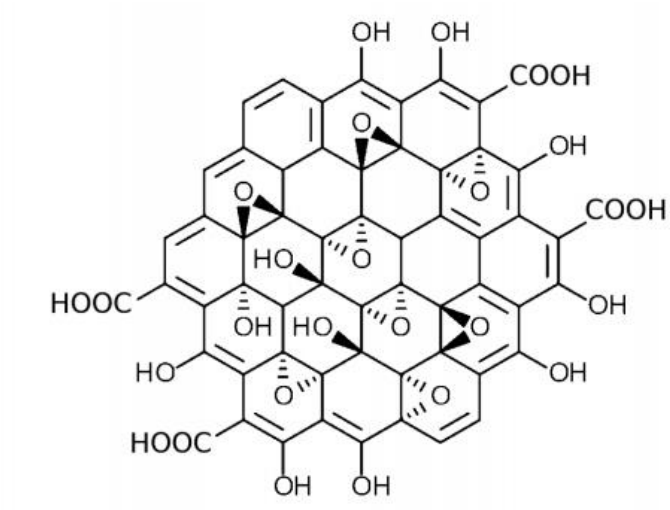

Fig. 1. Structure of GO according to Lerf-Klinowski model [35]

Covalent bonds exist between the previously mentioned oxygenated functional groups and carbon atoms in GO, resulting in oxidized sp^3 hybrids of carbons atoms that destabilize the non-oxidized regions of the original sp^2 honeycomb structure. As advantageous as the polar functional groups on GO, this also hinders GO by causing significant structural defects, reducing electrical conductivity and potentially restricting its direct application in electrically active materials and devices. It may also degrade the electronic, mechanical and electrochemical properties of GO. The non-specific binding that emerges with plane graphene sensors can be remedied by this covalent functionalization of specific molecules. Several techniques have been proposed to reduce the drawbacks of GO while maximizing the benefits of graphene properties [8]. Covalently bonding various chemical linkers of GO will change the graphene surface and refine its properties. In a case of electrochemical sensing application, GO functionalization improves its conductivity, selectivity and stability while also increasing sensitivity by increasing surface area.

GO can be functionalized by covalent binding, non- covalent binding modification and also by elemental doping [9]. GO can be modified according to the characteristics needed. This functionalization categorization based on structural features of GO. Covalent modification often damages parts of the graphene conjugation thereby jeopardizing some of its properties [9]. Non- covalent modification on the other hand is better because it maintains natural structure and properties of GO, it includes $\pi - \pi$ interaction and van der Waals force [9].

Non-covalent functionalized GO with aromatic compounds and nucleobase via $\pi - \pi$ stacking results in GO based biosensor that is capable of detecting DNA and proteins [9].

GO can be additionally functionalized with epoxy-group. Epoxide ring is opened by nucleophilic substitution at alpha carbon using an amino group to catalyze the reaction. The opening of epoxide ring results in a chemically converted graphene oxide sheet which is in form of a colloidal suspension. The suspension can be used as coating or reduced into high quality chemically modified graphene films. These attributes make it an excellent starting material for electrochemical sensors [10].Also, GO can be additionally functionalized with hydroxyl groups. For this purpose, GO surface is modified by silanization. Silanization is a process that coats a surface with surface with organofunctional alkoxysilane molecules; hydroxyl groups attacks and replace silane. EDTA – silane functionalized rGO/Nafion film coated on a glassy carbon electrode can be used to detect dopamine via oxidation [10].

1.2. Carbon based electrode materials

Solid metal electrodes have a smaller potential spectrum than carbon-based materials. The primary criteria for a good electrode material include long-term stability, low residual current, and a broad potential range. Graphite, carbon fibers, porous carbon, and glassy carbon, nanotubes and carbon spheres are all carbon - based materials that could be used as electrochemical transducers. These materials improve the efficiency of enzyme immobilization while also exhibiting repeatable electrochemical properties and consistent physical properties. The most popular carbon-based electrodes are glassy carbon electrodes. Glassy carbon a complex solid that's inherently stable, impermeable to gases and fluids, and chemically resistant in a variety of environments. It's easy to set up, polish, and clean, and it's safe to use with most solvents. The amplification of the performance of glassy carbon depends on polishing material used and thermal activation. They both increase the electron transfer rate and adsorption. Furthermore, this material's high porosity, low background current over a broad potential range, and wide functionality make it suitable for the adsorption of large molecules while also suggesting its potential use as an electrochemical transducer. The poor sensitivity of this material to peroxide and other mediators is one of its disadvantages when used in biosensor design [11].

Due to their high electrical conductivity, large surface area and exceptional durability, graphene-based materials have demonstrated great potential as electrode materials. In an attempt to modify the electrochemical properties of graphene-based electrodes, it can be doped with chemicals having electron donors and acceptors e.g. boron, nitrogen, oxygen, sulphur and phosphorus. Amidst the heteroatoms listed, nitrogen-doped carbon-based nanomaterials have outperformed other electrode materials in electrochemical measurements.

1.3. Biological activity of hydrogen peroxide

H_2O_2 is a small, relatively stable, and easily dissipated molecule. H_2O_2 is a poor oxidizing or reducing agent. It does not effectively oxidize most biological molecules, including lipids, DNA, and proteins except in the case of protein having hyperreactive thiol groups or methionine residues. The danger of H_2O_2 stems primarily from its easy conversion to reactive hydroxyl radical (OH), which can occur either by exposure to ultraviolet light or by reactions with a wide range of transition metal ions, the most relevant of which is potentially iron in vivo [12]. H_2O_2 can, indeed, be harmful to the body at high levels, causing cell damage, inflammatory disease, and cancer [6]. H_2O_2 is produced by many cells

and can be found in urine, blood, and exhaled air. As a result, measurements of H_2O_2 in body fluids and/or exhaled air may be used as a biomarker of oxidative stress during physiological and pathological conditions, as well as to monitor therapeutic outcomes [12].

1.3.1. Formation of H_2O_2

H_2O_2 is formed in two ways: via enzymatic or chemical dismutation of superoxide ions, and via action of oxidases by a two-electron reduction of oxygen by certain oxidases. Peroxisomal oxidases that directly generate H_2O_2 include glycolate, D-amino, ureate, L-a-hydroxyacid, and fatty-acyl-CoA oxidases. Furthermore, H_2O_2 is produced by the enzymes monoamino oxidase and lysyl oxidase, which are found in the mitochondria and the extracellular space, respectively [13]. H_2O_2 is generated by lysyl oxidase, which is involved in the formation of aldehyde precursors of cross-links in collagen and elastin. This enzyme binds to collagen and elastin in the extracellular space and is important for the oxidation of ε-amino groups of specific lysyl and hydroxylysyl residues to produce aldehydes, which are needed for intra- and inter-chain cross-linking [13]. SOD is perhaps the only antioxidant enzyme that scavenges the superoxide anion by reducing it to oxygen and hydrogen peroxide, inhibiting the formation of peroxynitrite and subsequent damage. Many pathological processes in the body are strongly linked to free radicals [14]. The Fenton reaction can produce hydroxyl radicals when excess oxygen reacts with H_2O_2 [15] as demonstrated in figure 2.

1.3.2. Detoxification of H_2O

High levels of H_2O_2 (usually ≥50 μM) have shown to be cytotoxic to a plethora of animal, plant, and bacterial cells in culture. In vivo, H_2O_2 is extremely toxic and must be eliminated as quickly as possible [12]. There are several ways to detoxify H_2O_2 from the system, they are categorized into 3: antioxidant enzymes (catalase and glutathione peroxidase (GPX)); chain-breaking antioxidants (tocopherols and ascorbate); and transition metal-binding proteins (transferin and ferritin) [13].

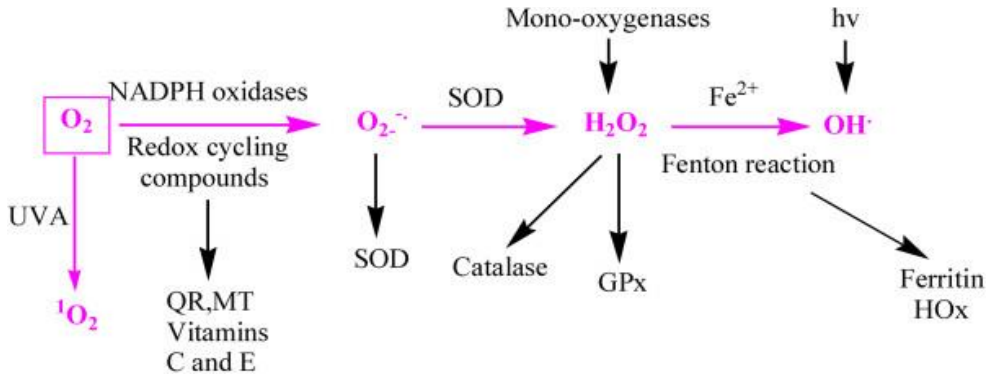

Fig. 2. Formation and detoxification of H_2O_2 [15]

As seen in figure 2, the superoxide radical anion (O_2-), hydrogen peroxide (H_2O_2), and the hydroxyl radical (OH•) are formed by successive reductions of the dioxygen molecule. To maintain the intracellular redox balance, antioxidants serve act as ROS scavengers. Quinone reductase (QR) detoxifies quinone compounds, while metallothionein (MT) binds to metal cations, vitamins C and E bind to free radicals. SOD and catalase dismutate superoxide (into oxygen and hydrogen peroxide) and hydrogen peroxide, respectively (into oxygen and water). Glutathione peroxidase (GPx) functions as catalase for peroxide compounds.[15]

- Glutathione peroxidase

  GPXs catalyze glutathione oxidation at the detriment of H_2O_2 or other hydroxyperoxides. GPX, like catalase, uses H_2O_2 as a substrate; however, unlike catalase, it can also react with lipids and other organic hydroxyperoxides. As a result, these enzymes play a vital role in preventing lipid peroxidation in cells [13]. This enzyme can be found in cytosol and mitochondria.

- Catalase

  Catalase is a heme-containing enzymatic complex which has peroxidase activity and reacts effectively with H_2O_2 to form H_2O and molecular oxygen as well as with H+ donors (methanol, ethanol, formic acid, phenols). It is mostly found in peroxisomes [13].

- Chain breaking antioxidants

  Vitamin E is a lipid-soluble compound that occurs naturally in the body with $\propto$-tocopherol being the most abundant. It is a membrane-bound chain-breaking antioxidant that protects cell membrane lipids from free radical oxidation. Because the excess charge associated with the extra electron is dispersed across the chromanol ring which is resonance stabilized, the resulting tocopheroxyl radical is relatively stable but can be further oxidized to from tocopherol quinone [13]. Ascorbate (vitamin C) is a free radical scavenger. This compound degrades hydroxyl and peroxyl radicals, as well as O_{2-} and nitrogen dioxide, hypochlorous acid, ozone, singlet oxygen, nitroxide, and peroxynitrite. Furthermore, it can reproduce other small-molecule antioxidants from their various radical species, such as a-tocopherol, glutathione, ureate, and b-carotene [13].

- Transition metal-binding proteins

  Metallothionein, ferritin, transferrin, and lactoferrin are common metalloproteins that serve as reservoirs for basic trace metals like copper and iron. These proteins are induced during the acute-phase response and under oxidative stress. These proteins reduce the harmful effects of ROS by inhibiting the redox-active metals iron and copper, reducing their ability to catalyze the Fenton reaction, which produces ROS [13]. These proteins reduce the harmful effects of ROS by inhibiting the redox-active metals iron and copper, reducing their ability to catalyze the Fenton reaction, which produces ROS.

1.3.3. H_2O_2 sensors

Due to the reactivity of H_2O_2 and its low physiological concentration, accurate identification is challenging, leading to uncertainty about the functions of H_2O_2 in the body. Titration, chromatography, light detection, and electrochemical sensors are among the many methods for detecting and quantifying H_2O_2 that have been in use. Although titration and chromatography can be used to measure H_2O_2 levels, they are inadequate for in vitro and in vivo studies. Light detecting sensors and electrochemical sensors are the two types of sensors extensively used to detect H_2O_2 in biological systems [16].

- Light detection sensors detect and analyze light emitted from a sample; however, their method of excitation, method of light modification, and emission wavelengths may all differ significantly. Chemiluminescence sensors use a chemical compound to change the H_2O_2, while fluorescence sensors rely on an external energy source, usually light. Sensors can work via changes in their emission profiles, such as a red or blue shift of peaks, as well as changes in emission intensity.[16]

- Electrochemical sensors

  Electrochemical sensors operate by using an electrical transducer to measure changes in chemical energy [16]. Because of their simplicity, low cost, high sensitivity, and selectivity, electrochemical techniques are recommended [17]. The theory behind amperometric sensors is that changes in current are proportional to changes in concentration [16]. Amperometric sensors measure the current while the potential (voltage) is preserved and it uses up to two or three electrodes to achieve this, whereas the potentiometric sensors measure the potential (voltage) between probes for which there is no current [17]. Potentiometric sensors include a reference electrode and a working electrode to calculate the electrical potential of an electrode while there is no noticeable current in the device. Electrodes with membranes surrounding their surface are calibrated to detect particular analytes [16]. The electrode will read the corresponding shift in electrical potential when the target analyte interacts with the membrane.H_2O_2 levels have been measured utilizing potentiometric and amperometric sensors [16]. Other electrochemical methods used to design H_2O_2 biosensors include cyclic voltammetry, linear sweep voltammetry, and differential pulse voltammetry [17]. Owing to their high sensitivity and selectivity, electrochemical techniques, especially enzyme-based sensors, have been developed for H_2O_2 monitoring. On the contrary, natural enzymes are responsive to their surroundings, so the instability of enzyme-based biosensors is unavoidable [19]. Other disadvantages of enzyme–based sensors include its price and its time-consuming immobilization procedure [18]. For the purpose of this study, nonenzymatic amperometric analysis of H_2O_2 was conducted. Advantages of this method includes high stability, simplistic handling, and a broad response range [18].

1.3.4. Electrode material for H_2O_2 detection

- Pt nanoparticles (Pt NPs) have been extensively used as an electrode material for the detection of H_2O_2 because of their excellent stability and good catalytic efficiency for H_2O_2 reduction. Wider electrochemically active surface areas can be achieved by coating graphene with metal nanoparticles, which effectively enhances electron transfer between electrode and detection molecules, resulting in a high sensitivity and specificity in current response [18]. Noble metals are well known for their excellent electrocatalytic behavior in H_2O_2 redox reactions. Pt NPs in particular have been widely

used as an exceptional electrocatalyst for the detection of H_2O_2 because their presence can generate a powerful electrocatalytic current for the transition of hydrogen peroxide and lower the H_2O_2 oxidation/reduction overvoltage which can easily prevent anodic interferents such as AA and UA [19].

- Other electrochemically active nanomaterials used for detecting H_2O_2 include gold and carbon nanotubes, which have been widely investigated as electrochemical sensors due to their high surface-to-volume ratios and catalytic activities.

- CuO nanomaterials, in particular, are one of the most promising candidates for active electrode materials due to their unique properties, such as high stability and good electrical properties. The limiting factor of CuO is its ease to oxidize in air or aqueous solution, most metallic CuO nanomaterials unstable for electroanalysis. Although this method is considered low-cost, it entails high temperatures, high pressure, complex additives, and a lengthy reaction time [20]. When CuO nanomaterials are used together with pencil graphite electrode (PGE), there is greater sensitivity to H_2O_2.

- CNTs have fascinating properties, including a high surface to volume ratio, superlight weight, high tensile strength, high electrical conductivity, and good thermal conductivity. These properties make CNT a remarkable nanomaterial with the prospect for a wide range of applications, particularly in the biomedical field [22]. Carbon nanotubes are also being used in the development of an H_2O_2 biosensor. Decorating the nanocomposite of MB-Sodium Dodecylsulfate (SDS) with MWCNTs offers the possibility of a very sensitive H_2O_2 biosensor [6]. The competent use of carbon nanotubes as "molecular wires" has enabled direct electron transfer between redox centers of enzymes and electrodes, resulting in the new mediator-free biosensor [21].

- Manganese dioxide (MnO_2) is an inorganic material that has the ability to catalyze the electrocatalytic reaction of H_2O_2. Biosensors capable of measuring H_2O_2 have been made using a selection of MnO_2 nanomaterials [23].

2. EXPERIMENTAL

2.1. Materials

All reagents and materials were of analytical grade or high purity. Graphite used for the synthesis of GO was extra pure grade (Merck). Sulphuric acid (H_2SO_4, ≥ 98%, Sigma Aldrich), sodium nitrate ($NaNO_3$, p.a., Sigma Aldrich) potassium permanganate ($KMnO_4$, ≥ 99% purity, Sigma Aldrich), hydrochloric acid (HCl, p.a., Sigma Aldrich), hydrogen peroxide (H_2O_2, 30%, p.a. POCH). NR, MG and CR were all supplied by Sigma Aldrich.

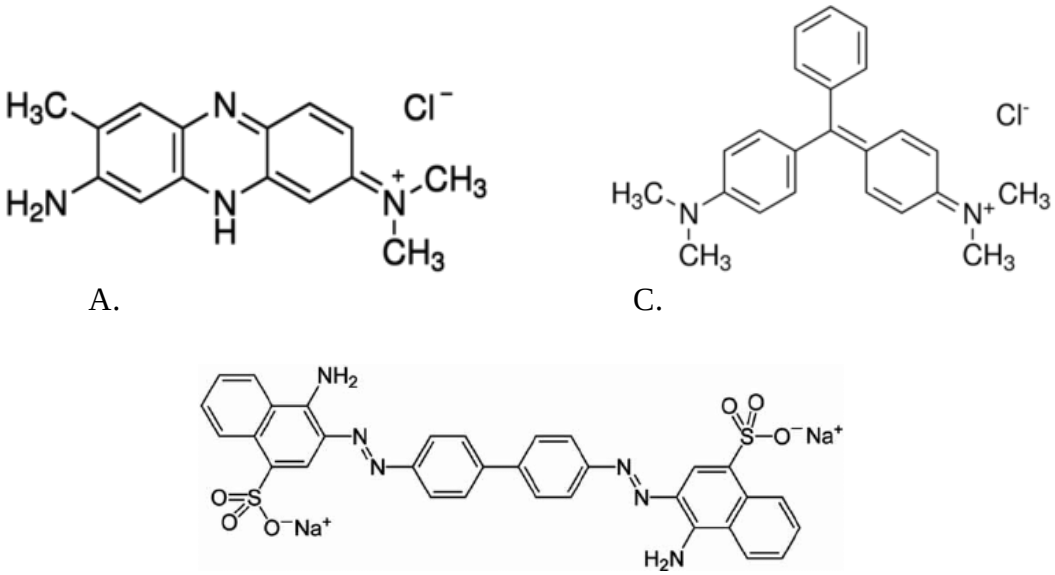

Fig. 3. Structures of a) Neutral red dye. b) Congo red dye. c) Malachite green dye [Sigma-Aldrich].

2.2. Methodology

2.2.1. Preparation of GO

GO was prepared using Hummer's method [24]. A beaker was placed in the middle of an ice bath. 240mLconcentrated H_2SO_4 was cooled to 3°C while constantly stirred with a magnetic stirrer. 3g of $NaNO_3$ was added while stirring for 10 minutes keeping the temperature at 5 – 6°C. 6.025g graphite powder was added in small amounts till fully incorporated while maintaining a temperature of 5 -6°C for about 10 minutes followed by subsequent gradual addition of 30g $KMnO_4$ in 10 – 15 minutes until exhausted. The reaction temperature was kept below 20^0C for this step. The reaction was heated at 55°C for 1hr while stirring. To the mixture, 276 mL deionized water was added in portions of 5ml slowly using an Eppendorf tube over a period of 1hr and by so doing, temperature is regulated at 60 – 70 °C. At the half portion mark of deionized water addition, the temperature starts to drop below the specification. The mixture is then heated up and maintained at 66 °C while adding the remaining deionized water at 15 minutes intervals. Furthermore, the mixture is added to 840mL deionized water and 25mL of 30% H_2O_2 while stirring. The mixture formed a bright yellow color as seen in figure 4, which was set aside to cool down. Upon cooling, the mixture was vacuum filtered and washed with 10wt% of HCl (1L) aqueous to remove metal ions.

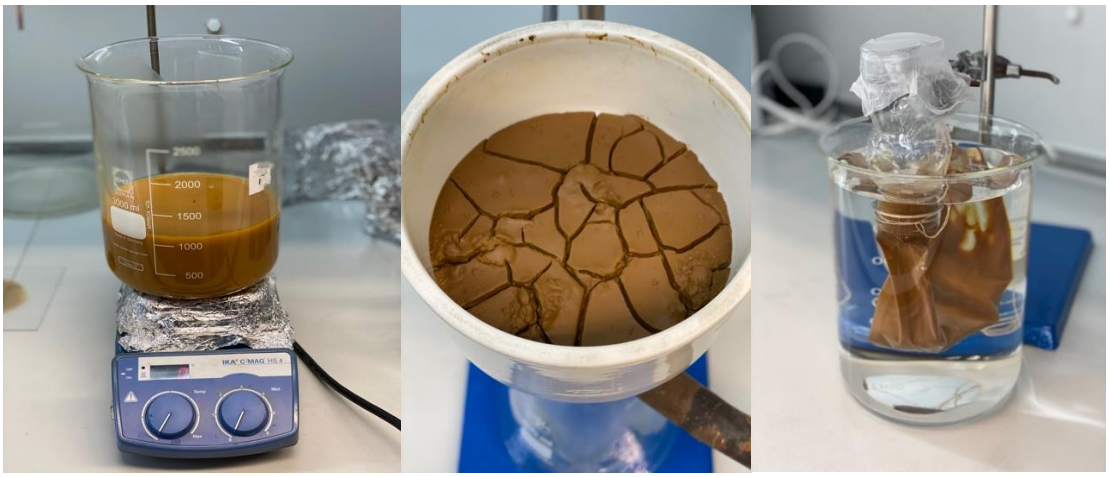

Fig. 4. Procedure of GO preparation. (a) Reaction mixture of GO after addition of H_2O_2. (b) GO after filtration. (c) GO suspension in the dialysis tube.

After filtration, the GO paste is mixed with a small amount if deionized water to form a suspension which is transferred carefully to a dialysis tubing membrane. The dialysis tube is submerged in a 3-liter beaker containing deionized water. Dialysis is done to remove sulphate ions and bring the pH value up to 6. To achieve this, the tub of deionized water was changed once daily for a period of 2 weeks to achieve this result. At pH of 6, the content of the dialysis tube was dried at room temperature to obtain GO powder.

2.2.2. Modification of GO with Dye

Three dyes namely Neutral red (NR), Malachite green (MG) and Congo red (CR) from three different classes of dyes (acridine, arylmethane and azo) respectively were used in the preparation of GO- dye nanocomposite. 20 wt% dye concentration was prepared. 0.125g of each dye was mixed separately with 0.1g GO after which it was filled up to 50mL with water in a volumetric flask to form a solution. Each dye mixture was sonicated for 1hr. After 1hr the dye mixture was poured in a Teflon lined autoclave then placed in a muffle oven at 180°C for 12hrs. The resulting sample was filtered, washed severally times with deionized water and allowed to dry at room temperature for a few hours as seen in figure 5.

Mass of the nanocomposite after reaction are as follows;
GO + MG = 0.2706g
GO + CR = 0.3275g
GO + NR = 0.3105g

Fig. 5. Modification of GO with dyes. (a) GO +MG after sonification. (b) Transfer of mixture into teflon autoclave. (c) Filtration of GO + MG.

3. CHARACTERIZATION

3.1. SEM

The samples' morphology and surface characterization were examined using a Hitachi SU-70 microscope at various magnifications and an accelerating voltage of 5.0 kV.

3.2. XPS

Analyses of X-ray photoelectron spectroscopy were carried out in a Kratos Axis Supra spectrometer using monochromatic Al K radiation (1486.69 eV). Binding energies were standardized in respect to the base C1s peak, which is 284.6 eV. The XPS spectra were deconvoluted by curve fitting peak components with the CASAXPS software without any pre-smoothing. Following a Shirley-type background subtraction, the fitting components' line shapes were approximated using symmetric Gaussian–Lorentzian product functions. Atomic ratios were measured using experimental intensity ratios and normalized using atomic sensitivity factors.

3.3. FTIR

FTIR measurements were performed in the range of 600 to 4000 cm^{-1} using a Frontier (PerkinElmer) FTIR spectrometer. The samples were made using the KBr pellet method. Sample powder (0.5 % by wt.) was combined with pure KBr powder for this experiment. Using a PIKE CrushIR hydraulic press with an 8 ton cm^{-2} pressure, the mixtures were pressed into transparent pellets for 5 minutes. A reference blank KBr pellet was used for calibration. All spectra were acquired from 100 scans with the spectral resolution of FTIR spectroscopes set at 4 cm^{-1}.

3.4. Raman spectroscopy

Raman spectra were obtained with an inVia Raman spectrometer (Renishaw, Gloucestershire, UK) outfitted with a thermoelectrically cooled (70 °C) CCD camera. An excitation beam at 532 nm with a power limit of 1 mW was provided to the He-Ne gas laser. The integration time was 100 s.

3.5. Electrochemical assessments

Electrochemical assessments of GO nanocomposites were performed using a custom-made analyzer (Vilnius University, Life Sciences Center, Lithuania) equipped with an electrochemical cell containing a three-electrode system consisting of an auxiliary platinum electrode, a reference Ag/AgCl electrode, and working (Ø 3.0 mm) electrode. The buffer used is 0.1M PBS (pH 7.2). The buffer was prepared by placing 28 mL NaH_2PO_4 and 72 mL $Na_2H_2PO_4$ in a volumetric flask, then filling it up to the 200 mL mark with deionized water. The final pH was adjusted to 7.2. The LOD and sensitivity of this study was calculated using the formulas [36] below.

$$LOD = 3 \times (\sigma / s). \quad \text{(Equation 1)}$$

$$Senstivity = s / A. \quad \text{(Equation 2)}$$

Where, σ is standard deviation of the response, s is slope of the calibration curve and A is surface area of the electrode.

4. RESULTS AND DISCUSSION

4.1. XPS Characterization

XPS was used to investigate the array of elements present in GO+NR, GO+CR, GO+MG and rGO. XPS analysis showed the presence of carbon, nitrogen, sulphur and oxygen. Deconvolution of their respective C1s spectrum indicates the presence of different types of carbon at different binding energy levels. The prominent peaks at 283 eV (C-C or C-H) and 284.7 eV signify sp^2 and sp^3 hybridized carbon respectively which strongly implies graphitic carbon. The other atoms present on the spectra include C-O or C-N (286 eV), C=O or C=N (287 eV), $\pi - \pi^*$(290 eV) and O-C=O (288 eV) [25]. The peak at 287.1 eV which corresponds to C-O/C-N shows a bond formation between dyes and GO in each respective C1s spectrum as shown in figure 6.

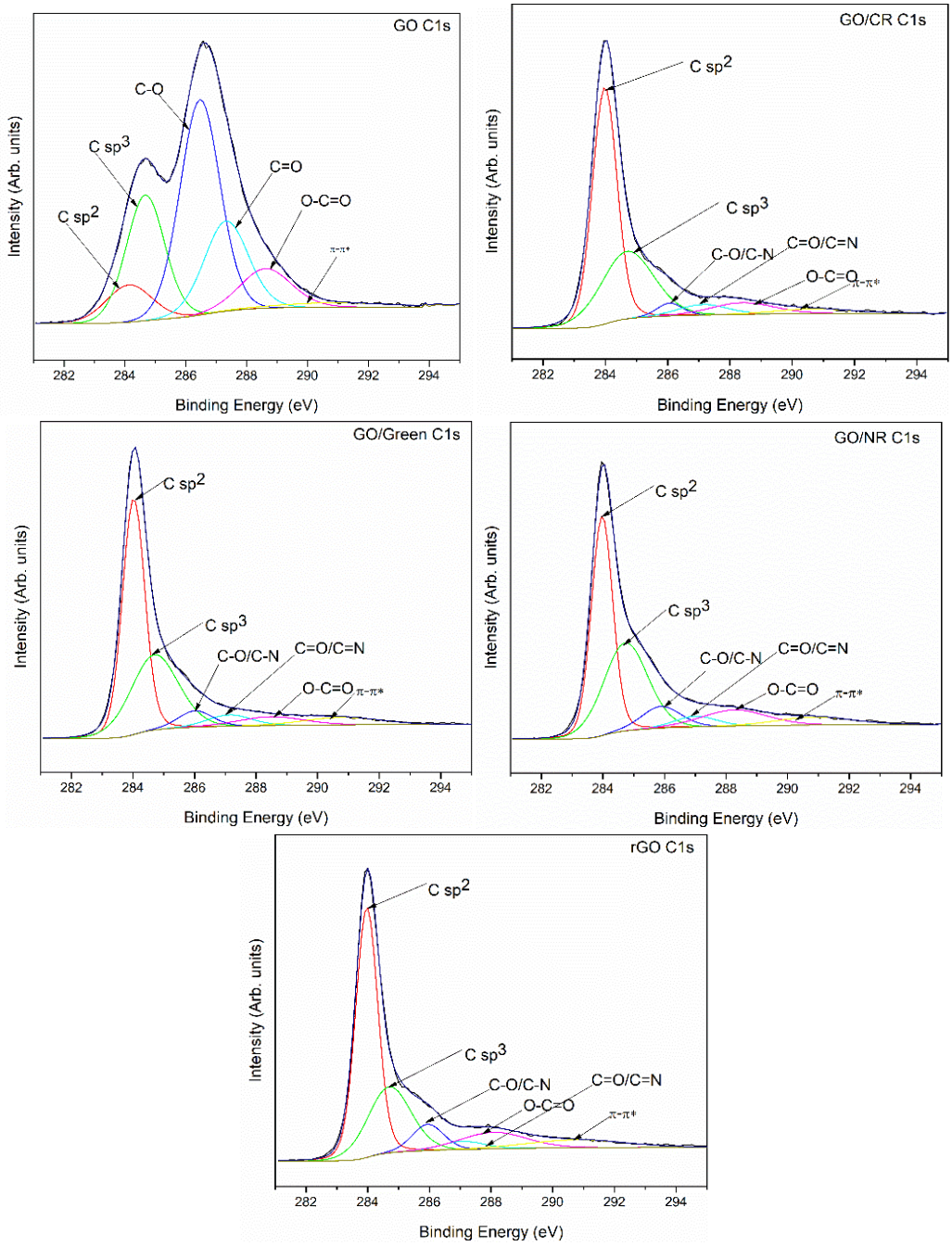

Fig. 6. XPS graph of C1s region of GO, GO nanocomposites and rGO.

The S2p spectrum is characterized by the binding energy at 168 eV which can be attributed to sulfate ions [26][27] as seen in figure 6.

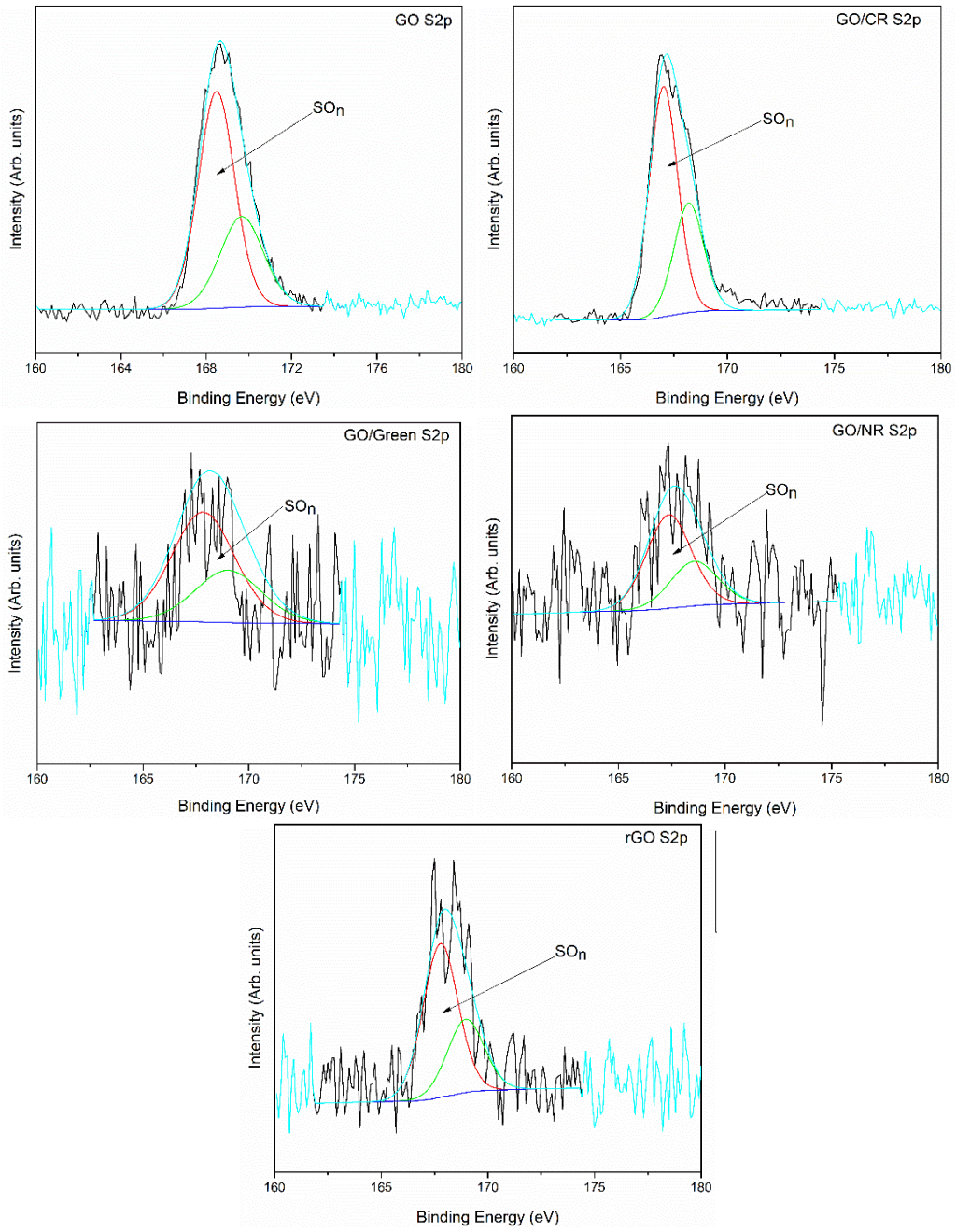

Fig. 7. XPS graph of S2p region GO, GO nanocomposites and rGO.

N1s peak was split into 3 peaks, the peak at 398.8 eV corresponds to imine (-N=), 399.5 eV represents amine (-NH-) while the peak at 400.5 eV likely indicates a positively charged nitrogen atom ($=N^{+}(CH_3)_2$ group [26] which can be explained by the presence aniline in NR and MG which are from sulphate ions [27] in dye structure in figure 7. The relative quantity of each element present in the above listed compounds is seen in table 1.

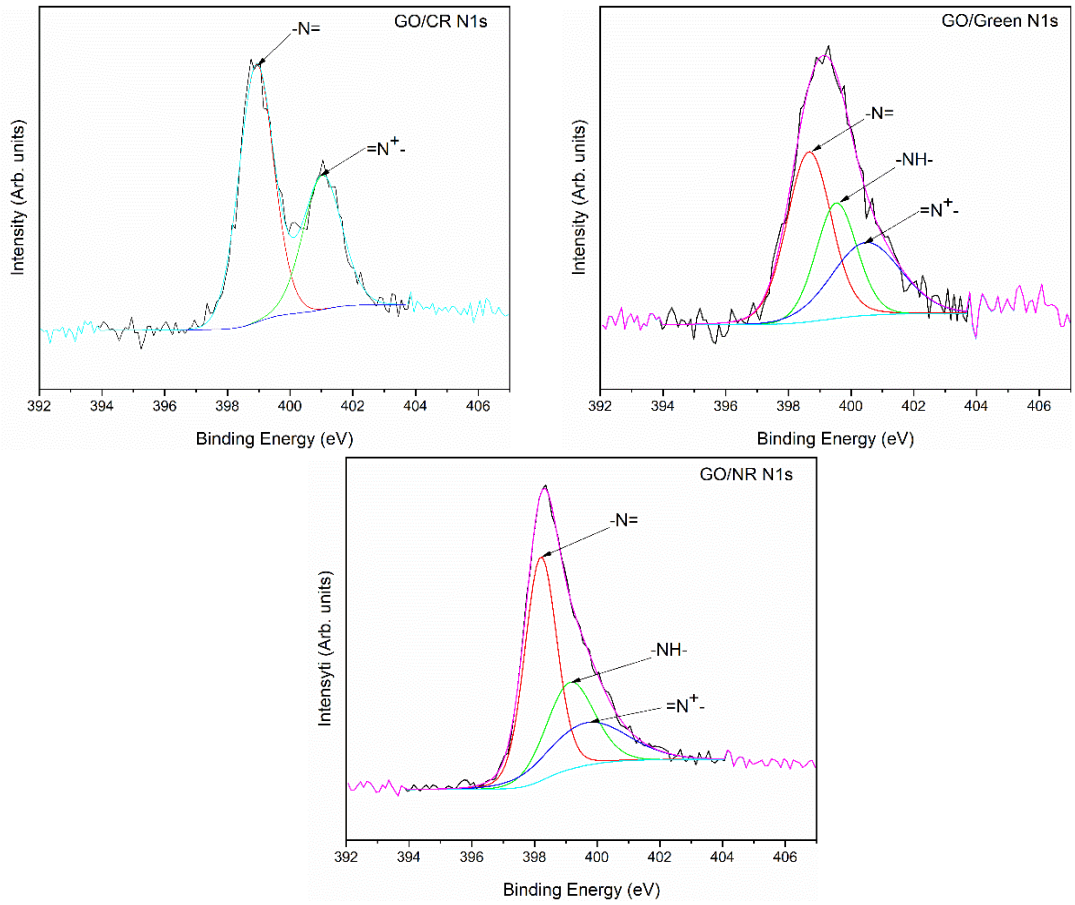

Fig. 8. XPS graph of N1s region of GO, GO nanocomposite and rGO

Table 1. Quantitative results of XPS analysis.

Sample	BE,[a] eV (Relative area, %)[b]									
	C1s						N1s			S2p
	Csp^2	Csp^3	C-O/ C-N	C=O/ C=N	O-C=O	π-π*	-N=	-NH-	$=N^+$-	$-SO_n$[a]
GO	284,2 (13,57)	284.7 (19,71)	286.5 (32,70)	287.3 (21,59)	288,6 (10,50)	291,0 (1,93)	n.d.	n.d.	n.d.	168,5 (100)
rGO	283,97 (49,34)	(284,7) 24,62	285,9 4 (7,09)	287.08 (2,97)	288.08 (9,38)	290,77 (6,59)	n.d.	n.d.	n.d.	168,96 (100)
GO/CR	283,98 (51,89)	284,7 (31,16)	286,0 6 (2,87)	287,13 (4,51)	288.40 (6,40)	290,73 (3,16)	398.9 2 (63.3)	n.d.	401.0 3 (36.7)	168,19 (100)
GO/MG	284.02 (48,43)	284.7 (31,95)	286,0 2 (5,01)	287.13 (4,47)	288.48 (5,10)	290,79 (5,05)	398.6 6 (17.31)	399,53 (40.07)	400,4 8 (42.63)	168,98 (100)
GO/NR	283,97 (41,48)	284.73 (33,3)	285.8 8 (7,26)	287,00 (3,83)	288,27 (8,96)	290.92 (5,18)	398.2 0 (20.38)	399,14 (43.89)	400,0 0 (35.73)	168.55 (100)

[a]For 2p orbitals the B.E. of 2p3/2 orbital is presented;
[b] Area of each component relative to the total core level peak area in percentage;
n.d. – not detected;

The presence of function groups on GO and its nanocomposite have been confirmed by XPS analysis as stated in table 1. High oxygen levels were detected in GO as a result of oxidation and low levels of oxygen in rGO as a result of reduction of GO. Residual sulfate ions are present in both GO and its nanocomposite from synthesis. Nitrogen groups can be seen in relatively large amount in GO/CR, GO/MG and GO/NR as a result of functionalization of dyes on GO.

4.2. FTIR Characterization

The structure and functional groups present in GO, rGO, GO+MG, GO+CR, and GO+NR were characterized by FTIR. The adsorption bands seen on GO spectra at 1725 cm^{-1}, 1621 cm^{-1}, 1396 cm^{-1}, 1059 cm^{-1} and the broad peak from 3653 – 3144 cm^{-1} indicate the presence of C=O stretch of carboxylic group, C=C groups, C-O stretch of carboxylic acid group, alkoxy C-O group and hydroxy -OH group respectively. The presence oxygen containing functional groups demonstrates the successful synthesis of GO while retaining graphite structure [28][29]. In GO-CR spectra, the intense peak at 1041 cm^{-1} signifies the S–O band and the peak position of the band is similar to CR compound. The sulfonate group does not participate in the adsorption of the CR molecule on the surface of the GO. The peaks seen around 1644 cm^{-1} in GO and GO nanocomposites is as a result of C=C vibrations in aromatic rings mixed with C=O stretching of ketone groups [30]. C-H stretching of amine is visible as small sharp peaks from

2924 - 2854 cm^{-1} in GO+MG, GO+CR and GO+NR [25]. The only significant peak in rGO is around 3625 – 3295 cm^{-1} which is due to O-H stretching [28]. The FTIR spectra as seen in figure 9a of rGO, GO and its nanocomposite easily demonstrates the reduction of GO and functionalization of dyes on GO. The FTIR spectra for pure dyes show prominent peaks at 1609 cm^{-1} - 1163 cm^{-1} are assigned to amines. For CR, the sulfonate group is 1048 cm^{-1} and 1586 cm^{-1} show aromatic ring for MG [30] as seen in figure 9b.

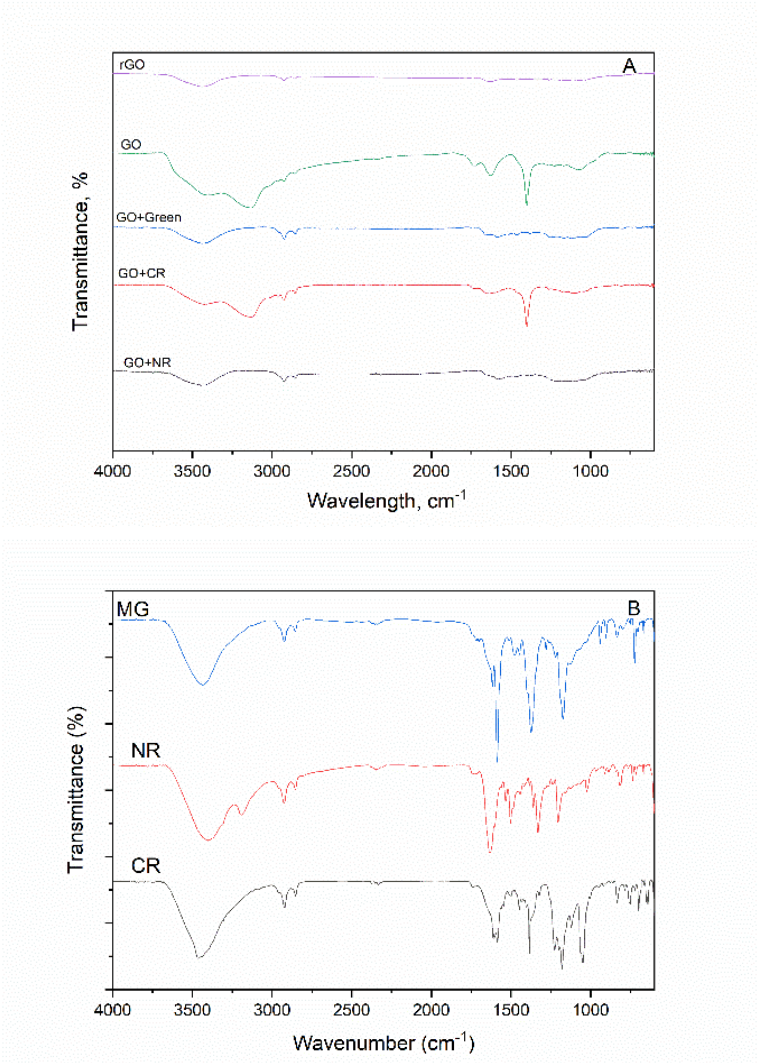

Fig. 9. FTIR spectra of a) rGO, GO and GO- dye nanocomposites. b) Pure dyes

4.3. Raman Characterization

Raman spectroscopy is a common and efficient technique for obtaining qualitative and quantitative information about the physical properties of graphene, such as crystallite size, structural defects, doping levels, and layer number. High Raman intensities are caused by conjugated and double carbon-carbon bonds [24][31]. In figure 10, the G-band at 1585 cm^{-1} corresponds to the E_{2g} phonon of the sp^2 C atoms, and a D band at 1346 cm^{-1} corresponds to the breathing mode of k- point phonons of A_{1g} symmetry in the standard Raman spectrum of GO [32]. Disorder is shown by the D band. The intensity ratios of D/G bands in each spectrum were used to determine the degradation state or oxidation level of GO [33]. GO

had a band intensity ratio of 1.0, while rGO, GO+CR, GO+MG, and GO+NR all had band intensity ratios of 0.85 to 0.83. The band intensity ratio decreases in rGO (0.84) compared to GO (1.0) indicates the removal of most oxygen containing functional group from GO [34].

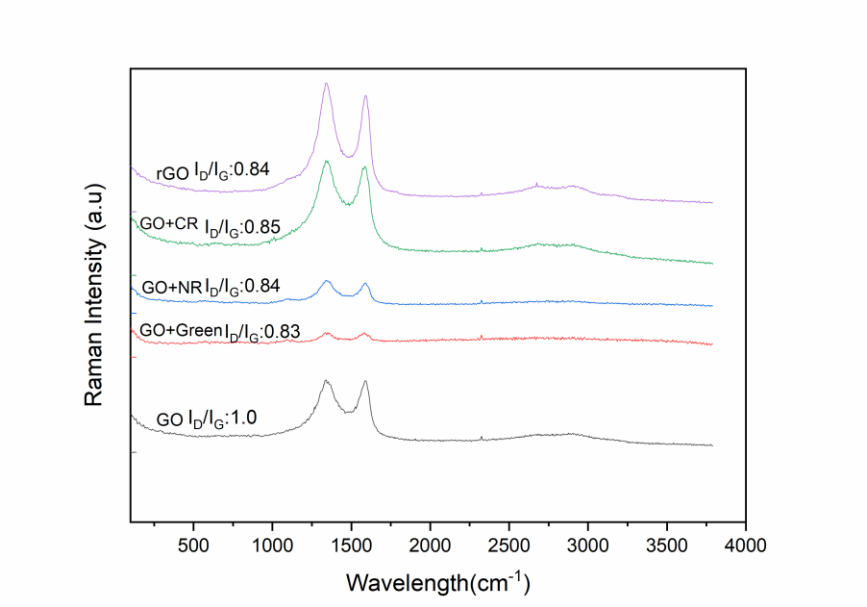

Fig. 10. Raman spectrum of GO and its nanocomposite.

4.4. SEM Characterization

SEM micrographs of GO flakes and layers indicate that they are in thin layers and have a wavy, folded structure. The SEM images also showed that the rGO is made up of clustered sheets that are closely linked. Our findings as seen in figure 11 indicate that the GO dispersion was created by thin layers of nanosheets [35]. showed a smooth surface morphology but a porous structure, implying that the chemical treatment process increased the surface roughness. This may be due to the chemical treatment separating the graphite layers into smaller sheets and it can be inferred that the chemical treatment increased the surface roughness [20]. These images were captured at different magnifications.

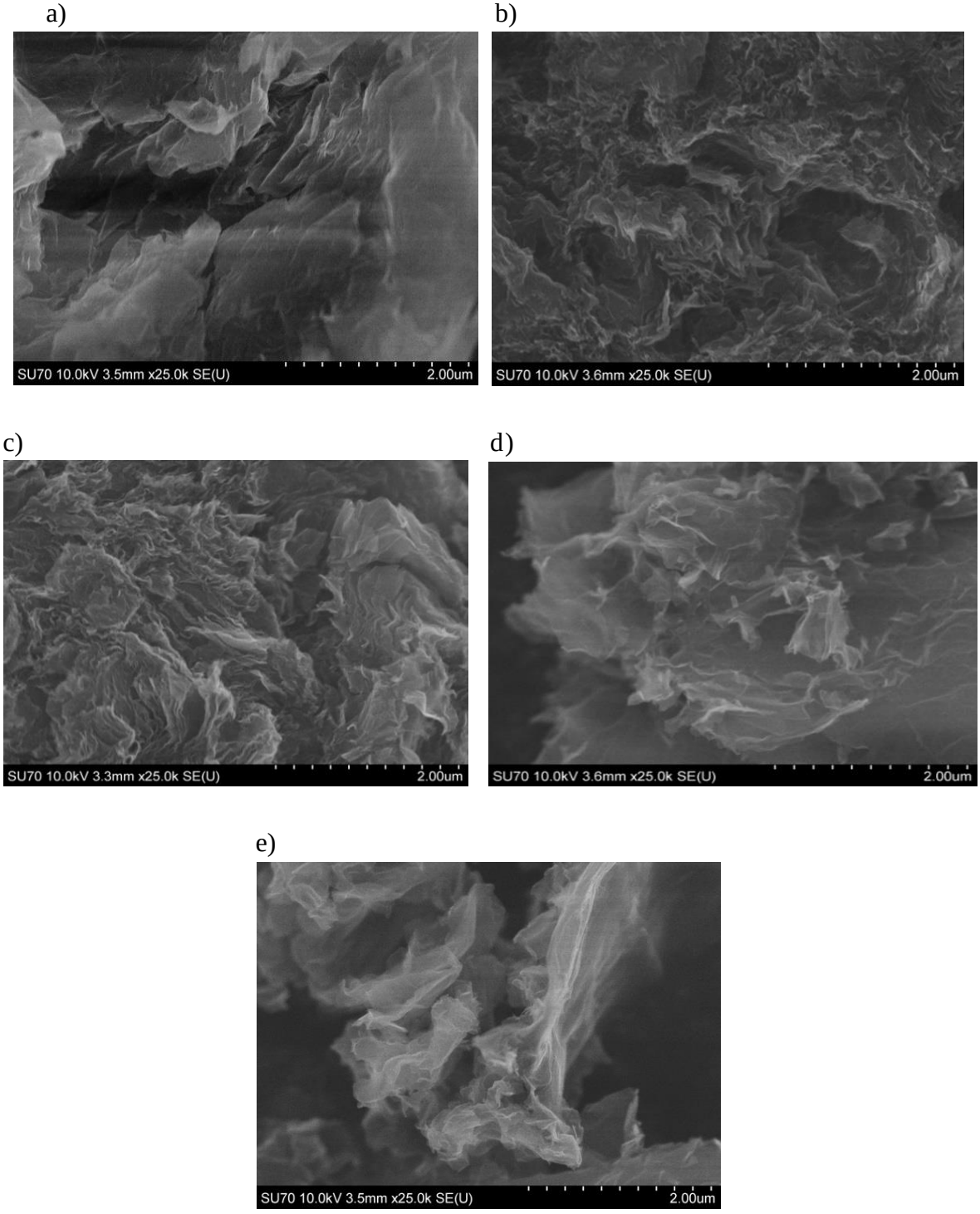

Fig. 11. SEM images of a) GO and b) rGO c) GO+CR d) GO+MG e) GO+NR

4.5. Electrochemical analysis of H_2O_2

A diagram of an electrochemical cell used in this study is depicted in figure 12. Figure 13 shows all the nanocomposites have both oxidative and reductive properties. This cyclic voltammetry was carried out using 0.01M PBS buffer, pH 7.2; 100 mM KCl; 1mM EDTA and 0.2mM H_2O_2. GO+MG had the highest anodic peak, thereby representing the best oxidation result at 832nA and 0.6 V. GO+NR showed the best reduction results at -349nA and -0.2V in comparison to GO+CR and GO+MG.

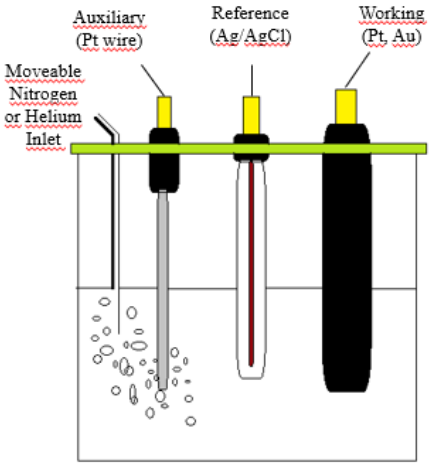

Fig. 12. Schematic diagram of electrochemical cell showing a reference, axillary electrode, electrolyte/ buffer, working electrode.

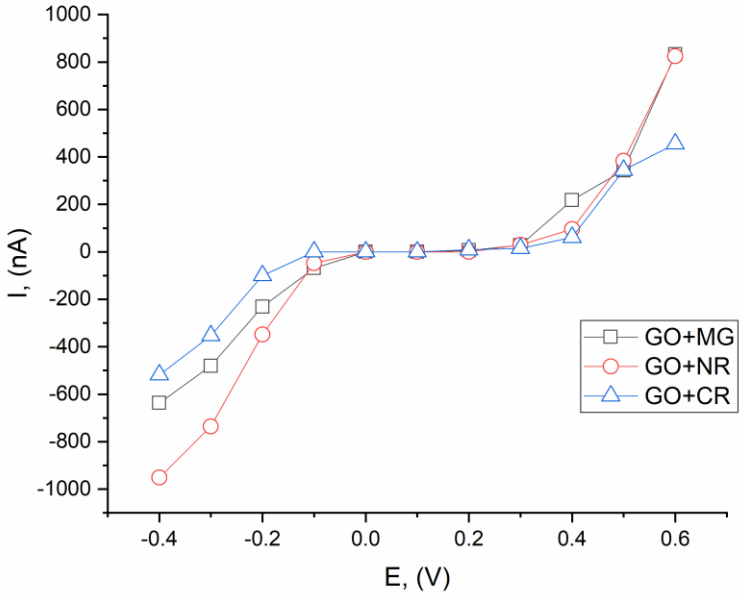

Fig. 13. Cyclic voltammogram of GO+NR, GO+CR, GO+MG in 0.01M PBS buffer, pH 7.2; 100mM KCl; 1mM EDTA and 0.2mM H_2O_2.

Table 2. Voltage vs current of GO+NR, GO+CR, GO+MG.

E (V)	GO+MG (nA)	GO+CR (nA)	GO+NR (nA)
-0.4	-637	-951	-518
-0.3	-481	-736	-353
-0.2	-231	-349	-100
-0.1	-69	-48	0
0	0	0	0
0.1	0	0	0
0.2	6	0	9
0.3	28	29	14
0.4	218	96	61
0.5	343	383	344
0.6	832	825	455

The amperometric response of GO+MG to the increasing amount of H_2O_2 is shown in figure 14a. The working potential was set at 0.6V and with each addition of H_2O_2 a rapid response showing steady state (95% maximum value) was attained within 5 seconds denoting rapid substrate diffusion in the film modified on the electrode and the sensor's high sensitivity to H_2O_2. The corresponding calibration curve for H_2O_2 in figure 14b depicts a sensitivity of 63.72 μA mM^{-1} cm^{-2} (r = 0.998) and a limit of detection of 0.049 mmol/L with signal to noise ratio of 3.

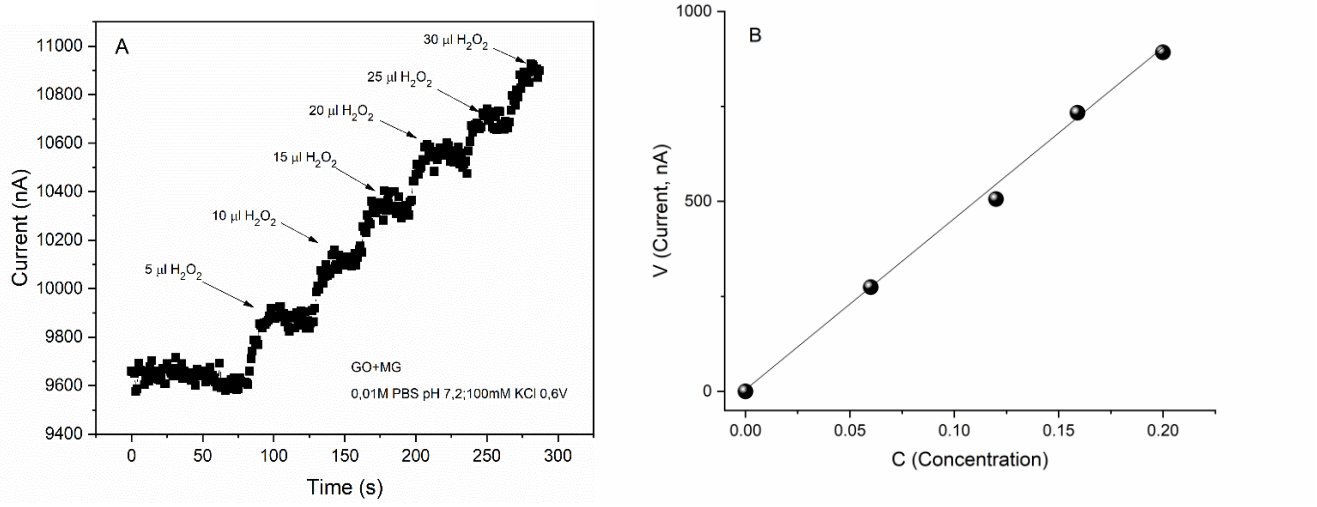

Fig. 14. a) Amperometric response of GO+MG/Pt electrode to successive addition of H_2O_2. b) calibration curve between current and concentration of H_2O_2 in 0.01M PBS (pH 7.2) with a working potential of 0.6V.

4.6. Reproducibility of biosensor

The measurement's reproducibility was determined by detecting 0.0121mM H_2O_2 five times with the same electrode as shown in figure 15. 12.52% was determined to be the coefficient of variation (CV). After the 4th run, current increased due to human error which can be explained by adding inaccurate amount of H_2O_2.

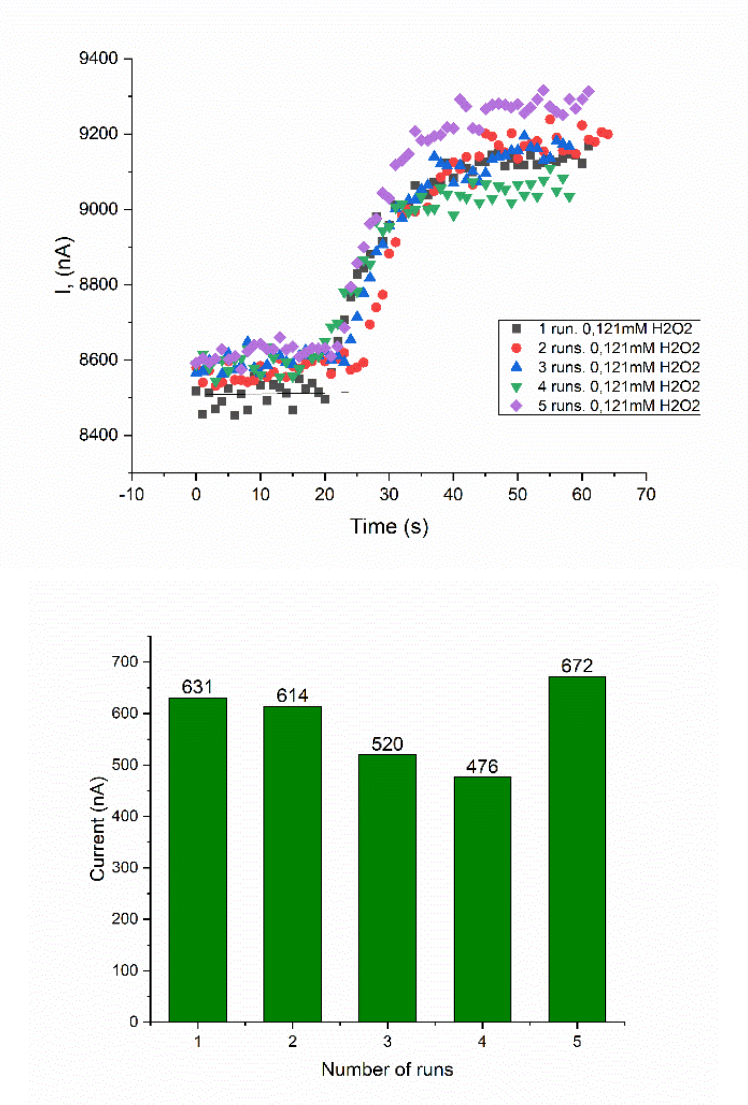

Fig. 15. Reproducibility graph and bar chart showing response of current to time and number of runs.

5. CONCLUSION

1. GO was successfully synthesized from graphite using Hummer's method. GO/dye (GO/congo red, GO/neutral red and GO/malachite green) nanocomposites were also synthesized.
2. Characterization performed by FTIR, XPS confirm the presence of oxygen containing groups, nitrogen, and sulphur on GO and its nanocomposites. SEM depicted structural changes in GO its nanocomposite and Raman spectroscopy indicated the extent of structural defect.
3. By deposition of MG on the surface of GO sheets in situ, a non-enzymatic sensor based on GO+MG was created. For H_2O_2 detection, the electrode has a strong electrocatalytic activity. We were able to achieve a low detection limit and a high sensitivity. As a result of the catalytic nature of MG towards H_2O_2 and the high surface area of GO, GO+MG provides opportunities for the development of non-enzymatic materials at low cost.

REFERENCE

1. H.C. Lee, W.W. Liu, S.-P. Chai, A.R. Mohamed, A. Aziz, C.S. Khe, U. Hashim, Review of the synthesis, transfer, characterization and growth mechanisms of single and multilayer graphene, RSC Advances. 7 (2017) 15644–15693. doi:10.1039/c7ra00392g.

2. S. Pei, H.M. Cheng, The reduction of graphene oxide, Carbon. 50 (2012) 3210-3228. doi:10.1016/j.carbon.2011.11.010.

3. K. Raidongia, A.T.L. Tan, J. Huang, Graphene Oxide: Some new insights into an old material, Carbon Nanotubes and Graphene. (2014) 341–374. doi:10.1016/b978-0-08-098232-8.00014-0.

4. A.K. Patel, N. Jain, P. Patel, R. Bajapi, Synthesis and application of Graphene Oxide (GO): A Review. International Journal for Scientific Research & Development. 4 (2016) 2321-613.

5. Y. Zhu, S. Murali, W. Cai, X. Li, J.W. Suk, J.R. Potts, R.S. V, Graphene and Graphene Oxide: synthesis, properties, and applications, Advanced Materials. 22 (2010) 3906–3924. doi:10.1002/adma.201001068.

6. L.J. Su, J.H. Zhang, H. Gomez, R. Murugan, X. Hong, D. Xu, Z.Y. Peng, Reactive Oxygen Species-induced lipid peroxidation in apoptosis, autophagy, and ferroptosis, oxidative medicine and cellular longevity. 2019 (2019) 1–13. doi:10.1155/2019/5080843.

7. A. Lerf, H. He, M. Forster, J. Klinowski, Structure of Graphite Oxide Revisited, J. Phys. Chem. 102 (1998) 4477−4482. doi:10.1021/jp9731821.

8. V. Georgakilas, M. Otyepka, A.B. Bourlinos, V. Chandra, N. Kim, K.C. Kemp, K.S. Kim, Functionalization of Graphene: Covalent and non-covalent Approaches, derivatives and applications, Chemical Reviews. 112 (2012) 6156–6214. doi:10.1021/cr3000412.

9. W. Yu, L. Sisi, Y. Haiyan, L. Jie, Progress in the functional modification of graphene/graphene oxide: a review, RSC Advances. 10 (2020) 15328–15345. doi:10.1039/d0ra01068e.

10. R. Hajian, K. Fung, P. Chou, S. Wang, S. Balderston, K. Aran, Properties and applications of functionalized Graphene Oxide. (2019). https://www.sigmaaldrich.com/technical-documents/articles/material-matters/functionalized-graphene-oxide.html (retrieved 24 May 2021).

11. A.D. Smith, Q. Li, A. Vyas, M.M. Haque, K. Wang, A. Velasco, X. Zhang, S. Thurakkal, A. Quellmalz, F. Niklaus, K. Gylfason, P. Lundgren, P. Enoksson, Carbon-based electrode materials for microsupercapacitors in self-powering sensor networks: Present and future development, Sensors. 19 (2019) 4231. doi:10.3390/s19194231.

13. B. Halliwell, M.V. Clement, L.H. Long, Hydrogen peroxide in the human body, FEBS Letters. 486 (2000) 1. doi:10.1016/s0014-5793(00)02197-9

14. M. Rojkind, J.A. Dominguez-Rosales, N. Nieto, P. Greenwel. Role of hydrogen peroxide and oxidative stress in healing process, Cellular and Molecular Life Science. 59 (2002) 1872-1891. doi:10.1007/PL00012511

15. F. Wang, Y.Q. Zhang, Bioconjugation of silk fibroin nanoparticles with enzyme and peptide and their characterization, protein and peptide nanoparticles for drug delivery. (2015) 263–291. doi:10.1016/bs.apcsb.2014.11.005

16. P. Shi, W. Sun, & P. Shi, A hypothesis on chemical mechanism of the effect of hydroge, Medical Gas Research. 2 (2012) 17. doi:10.1186/2045-9912-2-17

17. J. Meier, E.M. Hofferber, J.A. Stapleton, N.M. Iverson, Hydrogen peroxide sensors for biomedical applications, Chemosensors. 7 (2019) 64. doi:10.3390/chemosensors7040064

18. A.J.S Ahammad, Hydrogen Peroxide biosensors based on Horseradish Peroxidase and hemoglobin, J Biosens Bioelectron. (2013) 9. doi: 10.4172/2155-6210.S9-001.

19. Y. Zhang, X. Bai, X. Wang, K.K. Shiu, Y. Zhu, H. Jiang, Highly sensitive Graphene–Pt nanocomposites amperometric biosensor and its application in living cell H_2O_2 detection, Analytical Chemistry. 86 (2014) 9459–9465. doi:10.1021/ac5009699

20. Z. Bai, G. Li, J. Liang, J. Su, Y. Zhang, H. Chen, Y. Zhao, Non-enzymatic electrochemical biosensor based on Pt NPs/RGO-CS-Fc nano-hybrids for the detection of hydrogen peroxide in living cells, Biosensors and Bioelectronics. 82 (2016) 185–194. doi:10.1016/j.bios.2016.04.004.

21. M. Kamyabi, N. Hajari, Low potential and non-enzymatic hydrogen peroxide sensor based on Copper Oxide nanoparticle on activated pencil Graphite Electrode, Journal of the Brazilian Chemical Society. 28 (2016) 808-818. doi:10.21577/0103-5053.20160232.

22. K. Zhou, Y. Zhu, X. Yang, J. Luo, C. Li, S. Luan, A novel hydrogen peroxide biosensor based on Au–graphene–HRP–chitosan biocomposites, Electrochimica Acta. 55 (2010) 3055–3060. doi:10.1016/j.electacta.2010.01.035.

23. J. Ponmozhi, C. Frias, T. Marques, O. Frazão, Smart sensors/actuators for biomedical applications: Review, Measurement. 45 2012 1675–1688. doi:10.1016/j.measurement.2012.02.006.

24. L. Li, Z. Du, S. Liu, Q. Hao, Y. Wang, Q. Li, T. Wang, A novel nonenzymatic hydrogen peroxide sensor based on MnO2/graphene oxide nanocomposite, Talanta. 82 (2010) 1637–1641. doi:10.1016/j.talanta.2010.07.020.
25. G. Arthi, B. Paulchamy, B.D. Lignesh, A simple approach to stepwise synthesis of Graphene Oxide nanomaterial, Journal of Nanomedicine & Nanotechnology. 6 (2015) 2157-7439 . doi:10.4172/2157-7439.1000253.

26. C. Liu, Z. Xu, L. Liu, Covalent bonded Graphene/Neutral Red nanocomposite prepared by one-step electrochemical method and its electrocatalytic properties toward Uric acid, Electroanalysis. 30 2018 1017–1021. doi:10.1002/elan.201700817.

27. C. Chen, Y. Gao, Electrochemical characteristics of polyaniline electrosynthesized in the presence of neutral red, Materials Chemistry and Physics. 102 (2007) 24–30. doi:10.1016/j.matchemphys.2006.10.005.

28. F. Fusalba, D. Bélanger, Electropolymerization of Polypyrrole and Polyaniline−Polypyrrole from organic acidic medium, The Journal of Physical Chemistry B. 103 (1999) 9044–9054. doi:10.1021/jp9916790.

29. J. Song, X. Wang, C.T. Chang, Preparation and characterization of Graphene Oxide, Journal of Nanomaterials. 2014, 1–6. doi:10.1155/2014/276143.

30. M.B. Moraes, L. Cividanes, G. Thim, Synthesis of Graphene Oxide and functionalized CNT nanocomposites based on epoxy resin, Journal of Aerospace Technology and Management. 10 2018 3418. doi:10.5028/jatm.v10.944.

31. R. Trusovas, G. Niaura, J. Gaidukevič, I. Mališauskaitė, J. Barkauskas, Graphene oxide-dye nanocomposites: effect of molecular structure on the quality of laser-induced graphene, Nanotechnology. 2018. doi:10.1088/1361-6528/aadc85.

32. J. Guerrero-Contreras, F. Caballero-Briones, Graphene oxide powders with different oxidation degree, prepared by synthesis variations of the Hummers method, Materials Chemistry and Physics. 153 2015 209-220. doi:10.1016/j.matchemphys.2015.01.005.

33. F.T. Johra, J.W. Lee, W.G. Jung, Facile and safe graphene preparation on solution based platform, Journal of Industrial and Engineering Chemistry. 20 2014 2883-2887.doi:10.1016/j.jiec.2013.11.022.

34. R. Kurapati, F. Bonachera, J. Russier, A.R. Sureshbabu, C. Ménard-Moyon, K. Kostarelos, A. Bianco, Covalent chemical functionalization enhances the biodegradation of graphene oxide, 2D Materials. 5 2017 15020. doi:10.1088/2053-1583/aa8f0a.

35. S. Perumbilavil, P. Sankar, T.P. Rose, R. Philip, White light Z-scan measurements of ultrafast optical nonlinearity in reduced graphene oxide nanosheets in the 400–700 nm region, Applied Physics Letters. 107 (2015) 051104. doi:10.1063/1.4928124

36. D.R. Dreyer, C.W. Bielawski, Carbocatalysis: Heterogeneous carbons finding utility in synthetic chemistry, Chemical Science, 2 2011 1233. doi:10.1039/c1sc00035g

SUMMARY

VILNIUS UNIVERSITY
FACULTY OF CHEMISTRY AND GEOSCIENCES

SONIA ISHIOMA OKOLO

Study on The Structure and Electrocatalytic Activity Toward Hydrogen Peroxide of Graphene-Based Nanocomposite Materials Containing Organic Dyes.

For the nonenzymatic detection of H2O2, three novel electrocatalysts, GO+CR, GO+NR, and GO+MG nanocomposite, were effectively synthesized. Scanning electron microscopy, X-ray photoelectron spectroscopy, Fourier-transform infrared spectroscopy, and Raman spectroscopy were used to characterize. For the detection of H2O2, the GO+MG based electrodes demonstrated strong electrochemical activity. These findings show that this novel nanocomposite with a large surface area and electrocatalytic activity has a lot of potential for nonenzymatic sensor application.